Comp. Appl. Math.
https://doi.org/10.1007/s40314-018-0591-9

Layer potential approach for fast eigenvalue characterization of the Helmholtz equation with mixed boundary conditions

Matthieu Dupré[1] · Mathias Fink[1] · Josselin Garnier[2] · Geoffroy Lerosey[1]

Received: 9 January 2018 / Accepted: 5 February 2018

Abstract Our goal is to propose an efficient approach to characterize the eigenvalues and eigenfunctions of the Helmholtz equation with mixed (Dirichlet and Neumann) boundary conditions. Our approach is based on layer potentials. We extend the eigenvalue characterization known for Neumann boundary conditions to the case of mixed boundary conditions. The problem is motivated by the need of such methods for real-time wave-field shaping by electronically tunable surfaces.

Keywords Layer potential · Eigenvalue problem · Boundary integral equation

Mathematics Subject Classification 35B30 · 35P15

1 Introduction

Wave control in cavities is a fundamental issue of applied and fundamental physics, from microwave ovens, indoor wireless communication, electromagnetic compatibility, to masers, quantum electrodynamics, and quantum chaos (Hill 2009). As it becomes possible to tune the boundary conditions of a cavity, it is necessary to propose a fast and reliable method to compute the modes of the cavity, to optimize the boundary conditions for a prescribed goal, such as a hotspot at a target point and an open or closed channel at a given frequency. Our goal is to propose an efficient approach to characterize the eigenvalues (and eigenfunctions) of the Helmholtz equation with mixed (Dirichlet and Neumann) boundary conditions. Our approach is based on layer potentials. The eigenvalue characterization for Neumann boundary

Communicated by Cristina Turner.

✉ Josselin Garnier
josselin.garnier@polytechnique.edu

1 Institut Langevin, ESPCI ParisTech, CNRS UMR 7587, 1 Rue Jussieu, 75005 Paris, France

2 Centre de Mathématiques Appliquées, Ecole Polytechnique, 91128 Palaiseau Cedex, France

Published online: 26 February 2018

conditions is known (Taylor 1996); here, we extend the idea to Dirichlet and mixed boundary conditions.

A first motivation is the design of configurable cavities with tunable eigenmodes in acoustics. Let us consider a partially open acoustic cavity. The acoustic pressure (that is, the overpressure compared to the atmospheric pressure) should vanish at the open portions of the cavity, while its normal derivative should vanish at the hard portions of the boundary. The computations of the modes of the cavity amounts to determine the eigenvalues and the eigenstates of the Helmholtz equation with mixed boundary conditions. If several small doors can be manufactured in a closed cavity, and if these doors can be closed or open at will, then the control of these doors allows to design a configurable cavity with tunable eigenmodes. To get a prescribed distribution of eigenfrequencies, it is of interest to get a fast and reliable tool to estimate the eigenmodes of a cavity with mixed boundary conditions.

The second (and main) motivation is the real-time wave-field shaping in reverberating media in the electromagnetic domain. Indeed, the control of the eigenmodes of an electromagnetic cavity is a formidable challenge. The eigenmodes of a cavity are imposed by the geometry and type of the boundary conditions. However, up to recently, electromagnetic devices capable of switching from Dirichlet to Neumann conditions were not available. This explains why mechanical parts are ordinarily used to physically modify the properties of reverberant media: rotating trays in microwave ovens and mode stirrers in reverberation chambers. In Dupré et al. (2015), it is shown in the microwave domain that electronically tunable metasurfaces can locally modify the boundaries, switching them in real time from Dirichlet to Neumann conditions. This paves the way to the design of a “smart wall” as shown by Kaïna et al. (2014), which can be controlled electronically and that can modify the boundary conditions of a reverberation chamber, such as a room, to enhance the signal received at an antenna, such as a cell phone. The potential applications of this technique for enhanced indoor telecommunication are tremendous (see Kaïna et al. 2014; Hougne et al. 2016). To get a significant enhancement, it is necessary to use a “smart wall” with many controllable devices and to solve an optimization problem that requires estimating many times the Green’s function of the cavity, for different boundary conditions. That is why it is necessary to get a fast and reliable method to estimate the eigenmodes of a cavity whose boundary conditions are mixed.

A method based on the Lippmann–Schwinger equation was proposed in Luz et al. (1997), which can be applied with Dirichlet boundary conditions. However, this method fails for Neumann or mixed boundary conditions, because the problem cannot be written anymore as a Lippmann–Schwinger equation with a potential operator, as noticed in Martin (2003). In this paper, we propose a layer potential approach. The layer potential techniques have been developed first in the field of inverse problems (see Ammari and Kang 2004; Ammari et al. 2013). They are also efficient for solving not only boundary value problems, but also eigenvalue problems, in particular eigenvalue perturbation problems, under variations of domains or boundary conditions (Ammari et al. 2009). The eigenvalue characterization of a cavity with Neumann boundary conditions is known (Taylor 1996); here, we extend the idea to mixed boundary conditions.

The paper is organized as follows. We formulate the problem and introduce the single- and double-layer potentials for the Helmholtz equation in Sect. 2. We state the main result in Sect. 3. We discuss some numerical techniques and issues in Sect. 4. We finally propose some numerical result, comparing the results of the layer potential technique with full numerical simulations using Comsol in Sect. 5.

2 Formulation

Let Ω be a smooth bounded open domain in $\mathbb{R}^d$, $d = 2$ or 3. We use dimensionless units such that the size of the cavity is of order one and the speed of propagation is equal to one. The problem is to find the pairs of eigenvalues and eigenstates (in $L^2(\Omega)$) of

$$\Delta u(\boldsymbol{x}) + \omega^2 u(\boldsymbol{x}) = 0, \qquad \boldsymbol{x} \in \Omega, \tag{1}$$

with the mixed boundary conditions

$$u(\boldsymbol{x}) = 0, \quad \boldsymbol{x} \in \partial\Omega_D, \qquad \partial_\nu u(\boldsymbol{x}) = 0, \quad \boldsymbol{x} \in \partial\Omega_N, \tag{2}$$

where $\partial\Omega_N = \partial\Omega \backslash \partial\Omega_D$, $\partial\Omega = \bar{\Omega}\backslash\Omega$. We denote by $\boldsymbol{\nu}$ the outward unit normal vector and $\partial_\nu u(\boldsymbol{x}) = \lim_{t\to 0^+} \boldsymbol{\nu}(\boldsymbol{x}) \cdot \nabla u(\boldsymbol{x} - t\boldsymbol{\nu}(\boldsymbol{x}))$ for $\boldsymbol{x} \in \partial\Omega$.

We denote by Γ_ω the free space Green's function that is the fundamental solution of

$$\Delta\Gamma_\omega(\boldsymbol{x}) + \omega^2\Gamma_\omega(\boldsymbol{x}) = \delta_{\boldsymbol{0}}(\boldsymbol{x}), \quad \boldsymbol{x} \in \mathbb{R}^d,$$

subject to the Sommerfeld radiation condition or outgoing wave condition. If $d = 3$,

$$\Gamma_\omega(\boldsymbol{x}) = -\frac{\mathrm{e}^{i\omega|\boldsymbol{x}|}}{4\pi|\boldsymbol{x}|}.$$

If $d = 2$,

$$\Gamma_\omega(\boldsymbol{x}) = -\frac{i}{4} H_0^{(1)}(\omega|\boldsymbol{x}|),$$

where $H_0^{(1)}$ is the Hankel function of the first kind of order zero.

For a bounded smooth domain Ω in $\mathbb{R}^d$ and $\omega > 0$, let $\mathcal{S}_\omega$ be the "single-layer potential", that is, the linear operator defined for any $\phi \in L^2(\partial\Omega)$ by

$$\mathcal{S}_\omega[\phi](\boldsymbol{x}) = \int_{\partial\Omega} \Gamma_\omega(\boldsymbol{x} - \boldsymbol{y})\phi(\boldsymbol{y})\mathrm{d}\sigma(\boldsymbol{y}), \qquad \boldsymbol{x} \in \bar{\Omega},$$

and $\mathcal{D}_\omega$ be the "double-layer potential", that is, the linear operator defined for any $\phi \in L^2(\partial\Omega)$ by

$$\mathcal{D}_\omega[\phi](\boldsymbol{x}) = \int_{\partial\Omega} \frac{\partial\Gamma_\omega(\boldsymbol{x} - \boldsymbol{y})}{\partial\nu(\boldsymbol{y})}\phi(\boldsymbol{y})\mathrm{d}\sigma(\boldsymbol{y}), \qquad \boldsymbol{x} \in \Omega.$$

Properties of the single- and double-layer potentials can be found for instance in Ammari et al. (2013). In particular, they satisfy the trace relations (see also Colton and Kress 1992, Theorem 3.1):

$$\frac{\partial\mathcal{S}_\omega[\phi]}{\partial\nu(\boldsymbol{x})}(\boldsymbol{x}) = -\frac{\phi(\boldsymbol{x})}{2} + \mathcal{K}_\omega^*[\phi](\boldsymbol{x}), \qquad \text{for a.e. } \boldsymbol{x} \in \partial\Omega, \tag{3}$$

with

$$\mathcal{K}_\omega^*[\phi](\boldsymbol{x}) = \text{p.v.} \int_{\partial\Omega} \frac{\partial\Gamma_\omega(\boldsymbol{x} - \boldsymbol{y})}{\partial\nu(\boldsymbol{x})}\phi(\boldsymbol{y})\mathrm{d}\sigma(\boldsymbol{y}), \qquad \boldsymbol{x} \in \partial\Omega,$$

and

$$\mathcal{D}_\omega[\phi](\boldsymbol{x}) = \frac{\phi(\boldsymbol{x})}{2} + \mathcal{K}_\omega[\phi](\boldsymbol{x}), \qquad \text{for a.e. } \boldsymbol{x} \in \partial\Omega, \tag{4}$$

with

$$\mathcal{K}_\omega[\phi](\boldsymbol{x}) = \text{p.v.} \int_{\partial\Omega} \frac{\partial \Gamma_\omega(\boldsymbol{x}-\boldsymbol{y})}{\partial \nu(\boldsymbol{y})} \phi(\boldsymbol{y}) \mathrm{d}\sigma(\boldsymbol{y}), \qquad \boldsymbol{x} \in \partial\Omega.$$

Here, p.v. stands for the Cauchy principal value. The singular integral operators $\mathcal{K}_\omega^*$ and $\mathcal{K}_\omega$ are bounded on $L^2(\partial\Omega)$. The operator $\mathcal{K}_\omega^*$ is called the Neumann–Poincaré operator associated with the domain Ω.

3 Main result

If (ω, u) is a pair eigenvalue/eigenstate, then by the second Green's identity

$$\begin{aligned} &\int_\Omega \Delta_{\boldsymbol{y}} \Gamma_\omega(\boldsymbol{y}-\boldsymbol{x}) u(\boldsymbol{y}) - \Gamma_\omega(\boldsymbol{y}-\boldsymbol{x}) \Delta_{\boldsymbol{y}} u(\boldsymbol{y}) \mathrm{d}\boldsymbol{y} \\ &= \int_{\partial\Omega} \partial_\nu \Gamma_\omega(\boldsymbol{y}-\boldsymbol{x}) u(\boldsymbol{y}) - \Gamma_\omega(\boldsymbol{y}-\boldsymbol{x}) \partial_\nu u(\boldsymbol{y}) \mathrm{d}\sigma(\boldsymbol{y}), \end{aligned}$$

we have

$$u(\boldsymbol{x}) = -\mathcal{S}_\omega[\partial_\nu u](\boldsymbol{x}) + \mathcal{D}_\omega[u](\boldsymbol{x}), \qquad \boldsymbol{x} \in \Omega.$$

If we denote $\phi = u \mid_{\partial\Omega}$ (which is in $L^2(\partial\Omega)$ and is zero on $\partial\Omega_D$) and $\psi = \partial_\nu u \mid_{\partial\Omega}$ (which is in $L^2(\partial\Omega)$ and is zero on $\partial\Omega_N$), then we can write

$$u(\boldsymbol{x}) = -\mathcal{S}_\omega[\psi \mathbf{1}_{\partial\Omega_D}](\boldsymbol{x}) + \mathcal{D}_\omega[\phi \mathbf{1}_{\partial\Omega_N}](\boldsymbol{x}), \qquad \boldsymbol{x} \in \Omega. \tag{5}$$

Therefore, using the trace relations (3, 4), the functions ψ and ϕ must satisfy the following system of integral equations:

$$\frac{\psi(\boldsymbol{x})}{2} + \mathcal{K}_\omega^*[\psi \mathbf{1}_{\partial\Omega_D}](\boldsymbol{x}) - \frac{\partial}{\partial \nu(\boldsymbol{x})} \mathcal{D}_\omega[\phi \mathbf{1}_{\partial\Omega_N}](\boldsymbol{x}) = 0, \qquad \boldsymbol{x} \in \partial\Omega_D, \tag{6}$$

$$\frac{\phi(\boldsymbol{x})}{2} - \mathcal{K}_\omega[\phi \mathbf{1}_{\partial\Omega_N}](\boldsymbol{x}) + \mathcal{S}_\omega[\psi \mathbf{1}_{\partial\Omega_D}](\boldsymbol{x}) = 0, \qquad \boldsymbol{x} \in \partial\Omega_N. \tag{7}$$

The reciprocal is obvious: if (ϕ, ψ) satisfies the system (6, 7), then the function u defined by (5) satisfies the Helmholtz equation (1) and the mixed boundary conditions (2).

Accordingly, ω is an eigenvalue of the Helmholtz equation with mixed boundary conditions if and only if ω is a characteristic value of the linear system (6, 7), i.e., there exists a non-zero (ψ, ϕ) that satisfies the system.

For instance, for Neumann boundary conditions $\partial\Omega = \partial\Omega_N$, ω is an eigenvalue if and only if there exists a non-zero $\phi \in L^2(\partial\Omega)$ such that

$$\frac{\phi(\boldsymbol{x})}{2} - \mathcal{K}_\omega[\phi](\boldsymbol{x}) = 0, \qquad \forall \boldsymbol{x} \in \partial\Omega.$$

This is known in the literature (Taylor 1996). The characterization of the eigenvalues for mixed boundary conditions by the identification of the characteristic values of the system (6, 7) can be seen as an extension of this result.

4 Numerical implementation

The goal is to determine the characteristic values of the system (6, 7) that are the eigenvalues of the Helmholtz equation with mixed boundary conditions. The practical implementation requires discretizing the surface $\partial\Omega = \{\boldsymbol{x}_j,\ j = 1, \ldots, N\}$, together with the normal vector and the curvature at $\boldsymbol{x}_j$, and to use a quadrature formula (in dimension $d-1$) to approximate the integrals $\mathcal{K}^*_\omega[\psi](\boldsymbol{x}_l) = \sum_{j=1}^N K^*_{lj}\Psi_j$, $\Psi_j = \psi(\boldsymbol{x}_j)$ and $\mathcal{K}_\omega[\phi](\boldsymbol{x}_l) = \sum_{j=1}^N K_{lj}\Phi_j$, $\Phi_j = \phi(\boldsymbol{x}_j)$, as well as the single-layer potential and the normal derivative of the double-layer potential.

In the following, we consider the case $d = 2$.

The off-diagonal terms of the matrix $\mathbf{K}^*$ are:

$$K^*_{lj} = \frac{i\omega}{4} H_1^{(1)}(\omega|\boldsymbol{x}_l - \boldsymbol{x}_j|) \frac{(\boldsymbol{x}_l - \boldsymbol{x}_j)\cdot\boldsymbol{\nu}(\boldsymbol{x}_l)}{|\boldsymbol{x}_l - \boldsymbol{x}_j|}\sigma(\boldsymbol{x}_j)$$

where $\sigma(\boldsymbol{x}_j) = \frac{1}{2}(|\boldsymbol{x}_{j+1} - \boldsymbol{x}_j| + |\boldsymbol{x}_{j-1} - \boldsymbol{x}_j|)$ and we have used $H_0^{(1)\prime} = -H_1^{(1)}$. The diagonal terms can be computed by a limit and one finds

$$K^*_{jj} = \frac{\sigma(\boldsymbol{x}_j)}{4\pi r_j},$$

where r_j is the curvature of the surface at $\boldsymbol{x}_j$ and we have used the facts that $\frac{\partial\Gamma(\boldsymbol{x}-\boldsymbol{y})}{\partial\nu(\boldsymbol{x})} \simeq \frac{1}{2\pi}\frac{(\boldsymbol{x}-\boldsymbol{y})\cdot\boldsymbol{\nu}(\boldsymbol{x})}{|\boldsymbol{x}-\boldsymbol{y}|^2}$ for $\boldsymbol{y}$ close to $\boldsymbol{x}$ and $\frac{(\boldsymbol{x}-\boldsymbol{y})\cdot\boldsymbol{\nu}(\boldsymbol{x})}{|\boldsymbol{x}-\boldsymbol{y}|^2} \to \frac{1}{2r_x}$ as $\boldsymbol{y} \to \boldsymbol{x}$.

The elements of the matrix $\mathbf{K}$ have similar expressions: $K_{lj} = K^*_{jl}$.

The elements of the matrix $\mathbf{S}$ (for the the single-layer potential) are

$$S_{lj} = -\frac{i}{4} H_0^{(1)}(\omega|\boldsymbol{x}_l - \boldsymbol{x}_j|)\sigma(\boldsymbol{x}_j),$$

for $j \neq l$. The diagonal terms are

$$S_{jj} = -\frac{i}{4}\sigma(\boldsymbol{x}_j) + \frac{\sigma(\boldsymbol{x}_j)}{2\pi}(\ln\sigma(\boldsymbol{x}_j) + \gamma - 1),$$

with $\gamma \simeq 0.577$ the Euler's constant. Only the non-diagonal terms are relevant so far to get the field on $\partial\Omega$ in our approach as the matrix $\mathbf{S}$ couples Dirichlet boundary element to the Neumann boundary elements.

The elements of the matrix $\mathbf{D}'$ (for the normal derivative of the double-layer potential) are

$$\begin{aligned} D'_{lj} = &-\frac{i\omega^2}{4}\left(\frac{\boldsymbol{x}_l - \boldsymbol{x}_j}{|\boldsymbol{x}_l - \boldsymbol{x}_j|}\cdot\boldsymbol{\nu}(\boldsymbol{x}_l)\right)\left(\frac{\boldsymbol{x}_j - \boldsymbol{x}_l}{|\boldsymbol{x}_j - \boldsymbol{x}_l|}\cdot\boldsymbol{\nu}(\boldsymbol{x}_j)\right) H_2^{(1)}(\omega|\boldsymbol{x}_l - \boldsymbol{x}_l|)\sigma(\boldsymbol{x}_j) \\ &-\frac{i\omega}{4|\boldsymbol{x}_j - \boldsymbol{x}_l|}\boldsymbol{\nu}(\boldsymbol{x}_l)\cdot\boldsymbol{\nu}(\boldsymbol{x}_j) H_1^{(1)}(\omega|\boldsymbol{x}_l - \boldsymbol{x}_j|)\sigma(\boldsymbol{x}_j), \end{aligned}$$

for $j \neq l$. The diagonal terms are $D'_{jj} = \sigma(\boldsymbol{x}_j)/(8\pi r_j^2)$. Again, only the non-diagonal terms are relevant to find the field on the boundary $\partial\Omega$.

ω is an eigenvalue of the Neumann problem if the determinant of the matrix $\frac{1}{2}\mathbf{I}_{N,N} - \mathbf{K}_{N,N}$ is zero. (ω, ϕ) is an eigenvalue and eigenvector of the Neumann problem if $\boldsymbol{\Phi} = (\Phi_j)_{j=1}^N$ is an eigenvector of the matrix $\frac{1}{2}\mathbf{I}_{N,N} - \mathbf{K}_{N,N}$ with the eigenvalue 0.

ω is an eigenvalue of the Dirichlet problem if the determinant of the matrix $\frac{1}{2}\mathbf{I}_{N,N} + \mathbf{K}^*_{N,N}$ is zero. (ω, ψ) is an eigenvalue/eigenvector of the Dirichlet problem if $\boldsymbol{\Psi} = (\Psi_j)_{j=1}^N$ is an eigenvector of the matrix $\frac{1}{2}\mathbf{I}_{N,N} + \mathbf{K}^*_{N,N}$ with the eigenvalue 0.

ω is an eigenvalue of the mixed problem if the determinant of the matrix

$$\mathbf{W} = \begin{pmatrix} \frac{1}{2}\mathbf{I}_{N_D,N_D} + \mathbf{K}^*_{N_D,N_D} & -\mathbf{D}'_{N_D,N_N} \\ \mathbf{S}_{N_N,N_D} & \frac{1}{2}\mathbf{I}_{N_N,N_N} - \mathbf{K}_{N_N,N_N} \end{pmatrix} \tag{8}$$

is zero. (ω, ψ, ϕ) is an eigenvalue/eigenvector of the mixed problem if $((\Psi_j)_{j=1}^{N_D}, (\Phi_j)_{j=1}^{N_N})$ is an eigenvector of the matrix $\mathbf{W}$ with the eigenvalue 0. Here, $(\Psi_j)_{j=1}^{N_D}$ is the discretization of the normal derivative of the field on the Dirichlet boundary and $(\Phi_j)_{j=1}^{N_N}$ is the discretization of the field on the Neumann boundary.

To find the eigenvalues (which boils down to find the zeros of a function, the determinant of a large matrix), Muller's method is recommended in the literature, but it may be not necessary if the problem is simple. Muller's method is indeed an efficient interpolation method for finding a zero of a function defined on the complex plane (Stoer and Bulirsch 1993).

If the calculation of the determinant is impossible or too difficult or too costly, it is possible to look after the zeros of $1/[\boldsymbol{a} \cdot (\mathbf{W}^{-1}\boldsymbol{b})]$ for $\boldsymbol{a}$ and $\boldsymbol{b}$ two random complex vectors. This idea turns out to be quite efficient in practice and it has already been used in various contexts. Other randomized algorithms could be used as well (Halko et al. 2011).

Finally, once an eigenvalue ω has been identified, it is possible to get the corresponding eigenmode everywhere within the domain Ω by solving a discretized version of Eq. (5) that computes the field inside the domain from the field and its normal derivative at the boundary of the domain $\partial\Omega$ (given by $(\Phi_j)_{j=1}^{N_N}$, $(\Psi_j)_{j=1}^{N_D}$, respectively). Note that Eq. (5) allows to compute the eigenmode locally only, which is what is needed for the practical applications in which one wants to enhance the signal received by an antenna.

5 Numerical results

We restrict ourselves to a two-dimensional scalar case in acoustics and implement it with Matlab. The cavity is a rectangle of dimensions $L_x = 1$ m and $L_y = 2.3$ m. The medium is homogeneous with a speed of propagation $c_o = 343$ m s^{-1}, which corresponds to the celerity of sound in air. We test the layer potential technique and compare the results with the acoustics module of the commercially available finite element software Comsol multiphysics (using the eigenfrequency solver) for three configurations:

(1) full Neumann boundary conditions (Fig. 1),
(2) full Dirichlet boundary conditions (Fig. 2),
(3) mixed boundary conditions, with the 2.3 m long side with a Neumann boundary condition and the three other sides with Dirichlet boundary conditions (Fig. 3).

We look for the eigenvalues and eigenfunctions in the frequency band $[0, 400]$ Hz (which corresponds to wavenumbers up to 7.2 m^{-1}). The grid used for Comsol is made of triangular cells with a maximum size of $\lambda_0/10 \approx 0.08$ m, with λ_0 the smallest wavelength corresponding to the highest frequency. We apply our layer potential approach to a grid of rectangular elements of the same size $\lambda_0/10$.

We start by applying our method to the well-known case of full boundary Neumann condition, as is sketched on Fig. 1a. Figure 1b shows the modulus of the determinant of the matrix $\mathbf{W}$ defined sooner at Eq. (8). This already demonstrated approach is capable of distinguishing eigenvalues even when they are as close as a few Hz such as for the eigenfrequencies at 334.2 and 344.2 Hz. The zeros of the determinant correspond very well with the eigenfrequencies predicted with Comsol and marked by the vertical black lines and which correspond very

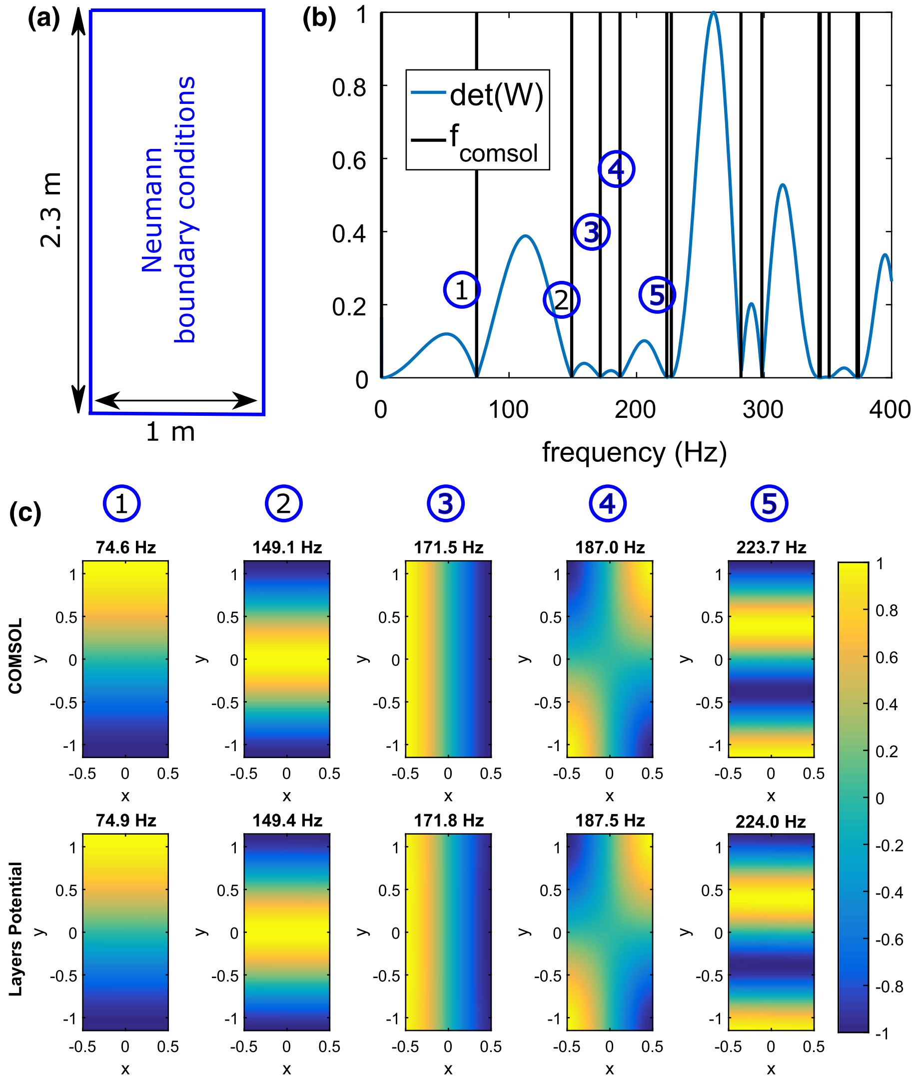

Fig. 1 Comparison between Comsol multiphysics and the boundary layers potential approach for Neumann boundary conditions. **a** Sketch of the cavity. **b** Modulus of the determinant of the matrix **W** as a function of the frequency, normalized by its maximum value. The vertical black lines show the eigenfrequencies predicted by Comsol. **c** Comparison of the first five eigenmodes of the cavity. The modes obtained with Comsol correspond to the acoustic pressure

accurately to the theoretical values (which can be computed here in this rectangular domain). Discrepancies between our approach and Comsol are less than 0.5% for the eigenvalues and less than 3% for the eigenmodes as seen in Table 1. Figure 1c plots the first five eigenmodes of the cavity obtained with Comsol and the boundary layer potential technique through Eq. (5) at the frequencies that cancel the determinant of **W**. The modes obtained with Comsol for the acoustic pressure are visually indistinguishable with the modes obtained with our approach.

We now apply our approach to full Dirichlet boundary conditions as shown in Fig. 2a. Figure 2b shows the modulus of the determinant of the matrix **W**. The zeros correspond very

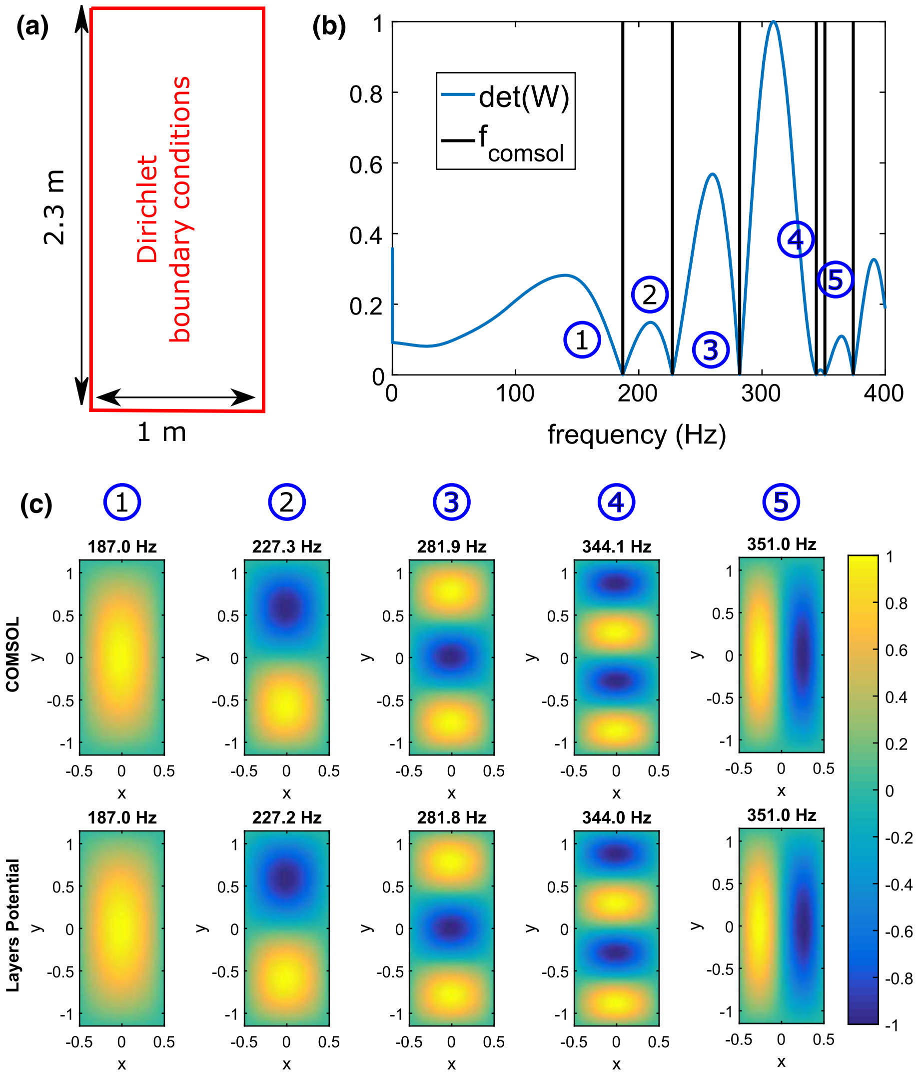

Fig. 2 Comparison between Comsol multiphysics and the boundary layers potential approach for Dirichlet boundary conditions. **a** Sketch of the cavity. **b** Modulus of the determinant of the matrix **W** as a function of the frequency, normalized by its maximum value. The vertical black lines show the eigenfrequencies predicted by Comsol. **c** Comparison of the first five eigenmodes of the cavity. The modes obtained with Comsol correspond to the acoustic pressure

well with the eigenfrequencies predicted with Comsol and marked by the vertical lines, and which correspond very accurately to the theoretical values. Again, the discrepancies between our approach and Comsol are very low as Table 1 shows. Figure 2c displays the first five eigenmodes of the cavity obtained with Comsol and the boundary layer potential technique. The modes obtained with Comsol for the acoustic pressure are visually indistinguishable with the modes obtained with our approach (less than 5% error). Those results validate the extension of the approach of the boundary layers potential to Dirichlet boundary conditions.

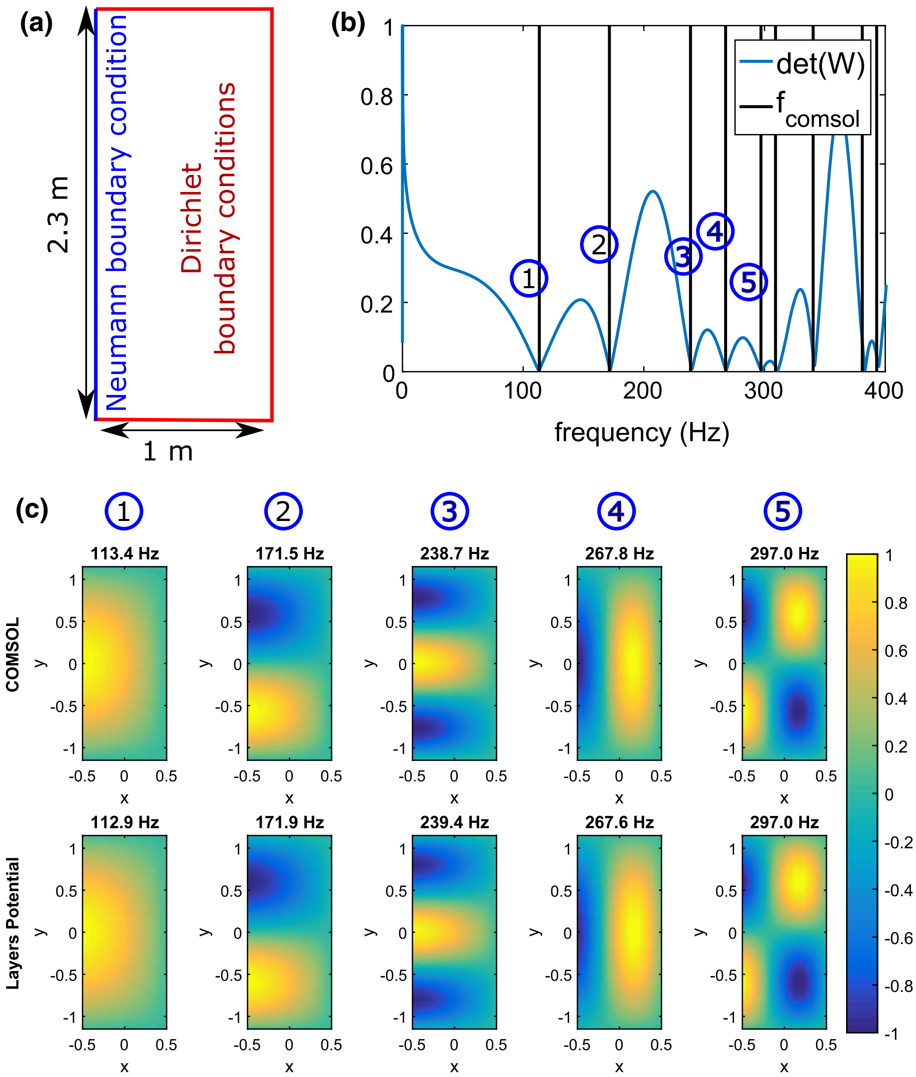

Fig. 3 Comparison between Comsol multiphysics and the boundary layers potential approach for mixed boundary conditions. **a** Sketch of the cavity. **b** Modulus of the determinant of the matrix **W** as a function of the frequency, normalized by its maximum value. The vertical black lines show the eigenfrequencies predicted by Comsol. **c** Comparison of the first five eigenmodes of the cavity. The modes obtained with Comsol correspond to the acoustic pressure

Finally, we apply our method to mixed boundary conditions. The long left side of the cavity is a Neumann boundary condition, while the three other sides are Dirichlet boundary conditions as can be seen in Fig. 3a. Figure 3b shows the modulus of the determinant of the matrix **W**. The zeros correspond with less than a 0.5% difference to the eigenfrequencies predicted with Comsol and marked by the vertical black lines. Figure 3c plots the first five eigenmodes of the cavity obtained with Comsol and the boundary layer potential technique. They spatially correspond to the even modes of a cavity with the double width, but restricted

Table 1 Comparing the differences between the eigenfrequencies and the eigenmodes obtained with Comsol and with the boundary layers potential method for the three different boundary conditions

Boundary conditions	Error	Mode #				
		1 (%)	2 (%)	3 (%)	4 (%)	5 (%)
Neumann	$\Delta\omega$	0.4	0.2	0.2	0.3	0.1
	Δu	2.2	2.5	2.5	2.7	3.3
Dirichlet	$\Delta\omega$	0.1	0.03	0.1	0.02	0.06
	Δu	1.8	5.4	3	5	0.2
Mixed	$\Delta\omega$	0.5	0.2	0.3	0.07	0.003
	Δu	2.3	2.1	2.6	2.9	3.6

$\Delta\omega = \left|\frac{\omega_{\mathrm{LP}}-\omega_{\mathrm{Com}}}{\omega_{\mathrm{Com}}}\right|$ and $\Delta u = \frac{||u_{\mathrm{LP}}-u_{\mathrm{Com}}||}{||u_{\mathrm{Com}}||}$ where $\|\cdot\|$ stands for the L^2-norm

to the domain of the current cavity. As in the cases with full Neumann and full Dirichlet boundary conditions, the eigenmodes of the acoustic pressure of a cavity with mixed boundary conditions obtained with Comsol are visually indistinguishable with the modes obtained with our approach. Discrepancies between our approach and Comsol are less than 0.5% for the eigenvalues and less than 3% for the eigenmodes as seen in Table 1. The slightly higher values for the differences of eigenmodes can be attributed to the interpolation errors between Comsol and our code. They can easily and quickly be reduced by increasing the mesh quality, if necessary. Remember that our goal was to show that it is possible to get the eigenvalues with high accuracy without solving the Helmholtz equation inside the domain accurately. Those results corroborate our approach and the extension of the potential layers to mixed boundary conditions.

6 Conclusion

In this paper, we have applied layer potential techniques to propose an efficient method to evaluate the eigenmodes and eigenfrequencies of a cavity with mixed boundary conditions. This method allows for fast calculations, which should help develop applications such as smart wall designs for improved indoor wireless performance. Such dynamic cavities have also found recent applications in microwave imaging to diversify the illumination patterns, which is relevant for security screening, through-wall imaging, biomedical diagnostics, and radar applications (Sleasman et al. 2016).

References

Ammari H, Garnier J, Jing W, Kang H, Lim M, Sølna K, Wang H (2013) Mathematical and statistical methods for multistatic imaging, vol 2098. In: Lecture notes in mathematics. Springer, Cham

Ammari H, Kang H (2004) Boundary layer techniques for solving the Helmholtz equation in the presence of small inhomogeneities. J Math Anal Appl 296:190–208

Ammari H, Kang H, Lee H (2009) Layer potential techniques in spectral analysis. AMS, Providence

Colton D, Kress R (1992) Inverse acoustic and electromagnetic scattering. Springer, New York

da Luz MGE, Lupu-Sax AS, Heller EJ (1997) Quantum scattering from arbitrary boundaries. Phys Rev E 56:2496–2507

del Hougne P, Lemoult F, Fink M, Lerosey G (2016) Spatiotemporal wave front shaping in a microwave cavity. Phys Rev Lett 117:134302
Dupré M, del Hougne P, Fink M, Lemoult F, Lerosey G (2015) Wave-field shaping in cavities: waves trapped in a box with controllable boundaries. Phys Rev Lett 115:017701
Halko N, Martinsson PG, Tropp JA (2011) Finding structure with randomness: probabilistic algorithms for constructing approximate matrix decompositions. SIAM Rev 53:217–288
Hill DA (2009) Electromagnetic fields in cavities: deterministic and statistical theories. Wiley, New York
Kaïna N, Dupré M, Fink M, Lerosey G (2014) Hybridized resonances to design tunable binary phase metasurface unit cells. Opt Express 16:18881–18888
Kaïna N, Dupré M, Lerosey G, Fink M (2014) Shaping complex microwave fields in reverberating media with binary tunable metasurfaces. Sci Rep 4:6693
Martin P (2003) Acoustic scattering by inhomogeneous obstacles. SIAM J Appl Math 64:297–308
Sleasman T, Imani MF, Gollub JN, Smith DR (2016) Microwave imaging using a disordered cavity with a dynamically tunable impedance surface. Phys Rev Appl 6:054019
Stoer J, Bulirsch R (1993) Introduction to numerical analysis, 2nd edn. Springer, New York
Taylor ME (1996) Partial differential equations II. Qualitative studies of linear equations. Springer, New York